Transcriptional regulation of the synthesis and secretion of farnesol in the fungus *Candida albicans:* Examination of the Homann transcription regulator knockout collection

Daniel J. Gutzmann*, Jaxon J. Kramer, Brigid M. Toomey, Cory H. T. Boone, Audrey L. Atkin* & Kenneth W. Nickerson*

School of Biological Sciences
University of Nebraska
Lincoln, NE USA

*For correspondence. E-mail : knickerson1@unl.edu, aatkin@unl.edu
daniel.gutzmann@huskers.unl.edu
Tel (402) 472-2253; Fax (402) 472-8722.

Keywords

- *Candida albicans*
- Farnesol
- Transcription factor mutant

Abstract

Candida albicans is an efficient colonizer of human gastrointestinal tracts and skin and is an opportunistic pathogen. *C. albicans* exhibits morphological plasticity and the ability to switch between yeast and filamentous morphologies is associated with virulence. One regulator of this switch is the quorum sensing molecule farnesol which is produced by *C. albicans* throughout growth. However, the synthesis, secretion, regulation, and turnover of farnesol is not fully understood. To address this, we used our improved farnesol assay to screen a transcription regulator knockout library of 164 mutants for farnesol accumulation in whole cultures, pellets, and supernatants. All mutants produced farnesol and they averaged 9.2X more farnesol in the pellet than the supernatant. Nineteen mutants had significant differences with ten mutants producing more farnesol than their $SN152^{+}$ parent while nine produced less. Seven mutants exhibited greater secretion of farnesol while two exhibited less. We examined the time course for farnesol accumulation in six mutants with the greatest accumulation differences and found that those differences persisted throughout growth and they were not time dependent. Significantly, two high accumulating mutants did not exhibit the decay in farnesol levels during stationary phase characteristic of wild type *C. albicans*, suggesting that a farnesol modification/degradation mechanism is absent in these mutants. Identifying these transcriptional regulators provides new insight into farnesol's physiological functions regarding cell cycle progression, white-opaque switching, yeast-mycelial dimorphism, and response to cellular stress.

62 **Introduction**

63 *Candida albicans* is an opportunistic pathogen that is present in most human gastrointestinal tracts and
64 is an efficient colonizer of mucosal surfaces (Neville et al. 2015). A weakened immune system (HIV,
65 chemotherapy, organ transplantation) or loss of competing flora (antibiotic treatment) allows for *C.*
66 *albicans* to colonize and invade host tissues leading to candidiasis (Pfaller and Diekema 2007). Virulence
67 of *C. albicans* is strongly linked to its ability to switch between yeast and filamentous morphologies
68 (Romano 1966; Kadosh 2019) as mutants that have lost the ability to switch are avirulent (Lo et al. 1997;
69 Saville et al. 2003). Dimorphism is also important for adaptation to different host environments (Noble
70 et al. 2017; Alves et al. 2020) and evading host immune responses (Gow et al. 2012). One regulator of
71 dimorphic switching is the quorum sensing molecule (QSM) farnesol (Hornby et al. 2001). Farnesol is
72 produced by *C. albicans* cells continuously throughout growth (Boone et al. 2022), except in
73 anaerobically grown cells (Dumitru et al. 2004) and opaque cells (Dumitru et al. 2007) where farnesol
74 production is much lower. However, despite numerous publications on farnesol's role as a QSM and
75 virulence factor, the actual mechanisms regulating its synthesis and secretion remain unclear.

76 As an approach to identifying these genes and mechanisms, we tested the hypothesis that
77 farnesol synthesis and secretion are regulated by the transcriptional networks involved in
78 morphogenesis and virulence. The transcription regulator knockout library generated by Homann and
79 colleagues has 165 different transcription regulators deleted, in most cases with two independently
80 derived knockouts (Homann et al. 2009). Thus, we grew each of the library strains in liquid culture and
81 then assayed them for total, extracellular, and intracellular farnesol by the improved methods of Boone
82 et al. (2022) . Key features of this assay include prevention of analyte loss by avoiding filtration and
83 minimizing evaporation, while incorporating simultaneous cell lysis and analyte extraction by ethyl
84 acetate. The assay enables comparison of whole culture values with the sum of their cell pellets and
85 supernatants. Our results suggest farnesol accumulation is integrated with transcriptional regulators of

86 cell cycle progression, white-opaque switching, yeast-mycelial dimorphism, and responses to cell stress.
87 Our results provide new insights into the physiological role of farnesol and understanding of the
88 regulatory mechanisms underlying its production.
89
90 **Materials and Methods**
91 **Strains and media**
92 The homozygous transcription regulator deletion mutants were obtained from the transcription
93 regulator knockout library provided by Dr. Alexander Johnson's lab (Homann et al. 2009) available
94 through the Fungal Genomics Stock Center (Manhattan, Kansas, USA; McCluskey et al. 2010). The strains
95 were maintained at 30°C on plates with YPD (1% yeast extract, 2% peptone, 2% glucose). The
96 transcription regulator knockout mutants were constructed from *C. albicans* SN152, an auxotroph for
97 arginine, histidine, and leucine. Each of the transcription regulator (TR) mutants is auxotrophic for
98 arginine. A wild-type control strain was created by reintroduction of a single allele of HIS1 and LEU2 into
99 the parent strain (Homann et al. 2009). Throughout this paper, we will refer to this control strain simply
100 as $SN152^{+}$. All assays with these mutants include the paired wild-type strain located in the H12 well of
101 the X2 and Y2 independently derived deletion collections.
102
103 **Screening the transcription regulator deletion mutants for differences in accumulation farnesol**
104 **secretion**
105 The transcription regulator mutant collection was transferred by a 48-pin replicator to YPD
106 plates and grown at 30°C for 48 hours. Mutants were then transferred to 3 mL YPD liquid medium and
107 grown for 16 hours at 30°C with rotary agitation at 250 RPM. This culture was used as the inoculum
108 (1:100) for 75 mL YPD in 250 mL flasks which were incubated 24 hours at 30°C, 250 RPM. Fifty mL of this
109 culture was used for dry weight determination and 20 mL (2 X 10 mL) was used for determination of

110 farnesol production as described by Boone et al. (2022). In this method, 10 mL was used to measure
111 whole culture values while the other was centrifuged to obtain the pellet and supernatant values. Due
112 to the large number of mutants in the collection, the mutants were assayed in batches of 10-20 mutants
113 with the $SN152^+$ control assayed in triplicate as part of each batch. Mutants with farnesol accumulation
114 of greater than 1 $\log_2$ fold above or below the mean value for $SN152^+$ were chosen for follow-up
115 analysis. In follow-up analyses, E,E-farnesol accumulation was measured in at least three independent
116 experiments using both the X and Y independently-derived TR deletion mutants (n=6).
117

118 **Temporal dynamics of farnesol accumulation**

119 To examine the time course of farnesol production, we assayed the farnesol accumulation of the
120 four highest and two lowest accumulating mutants at several cell densities throughout growth. Mutants
121 were inoculated into to 6 mL YPD liquid medium and grown for 16 hours at 30°C with rotary agitation at
122 250 RPM. This culture was used as the inoculum (1:100) for replicate flasks for each time point with 75
123 mL YPD per mutant strain. Farnesol measurements were taken 12, 18, 24, 36, 48, and 80 hours post
124 inoculation as describe by Boone et al. 2022. Two independent time courses were performed for the
125 mutant strains and three independent time courses were performed for the $SN152^+$ control. Farnesol
126 accumulation values were normalized to the 50 mL dry weight at the indicated time point. To quantify
127 differences in farnesol accumulation across time, area under the curve (AUC) analyses were performed
128 in GraphPad Prism.
129

130 **Statistical analysis**

131 Statistical analyses were performed using Microsoft Excel (Version 16.61, Microsoft Office, Las
132 Vegas, NV, USA) and GraphPad Prism Software (Version 9.5.0, San Diego, CA, USA). All biological data
133 are represented as mean $\pm$ SD of at least 3 biological replicates for both the X and Y independent

134 mutants unless otherwise stated. Mutants with significant differences between the X and Y mutant were
135 excluded and considered a false positive. Normality and homogeneity of variance were assessed by the
136 D' Agostino-Pearson omnibus (K2) test and Brown-Forsythe test, respectively. Differences between
137 groups that were normally distributed and homoscedastic (equal variances) were assessed by One-way
138 ANOVA with Dunnett's multiple comparisons test. Differences between groups that were not normally
139 distributed or heteroscedastic were assessed by the Kruskal-Wallis test with Dunn's multiple
140 comparisons tests. Both analyses were performed in GraphPad Prism. Differences were considered
141 significant at $p<0.05$ (*$p<0.05$, **$p<0.01$, ***$p<0.001$).

142 **Results**

143 **General design and reproducibility of the screen for farnesol regulators**

144 Homann et al. (2009) screened their collection of 165 independent transcription regulator mutants
145 for possible differences in 55 growth conditions. It was a monumental piece of work. However, for
146 practical reasons they limited themselves to phenotypes discernible via colonies on agar plates. We
147 have now extended the list of phenotypes to include accumulation of both intracellular and extracellular
148 farnesol as determined by our improved GC assay (Boone et al, 2022). For the initial screen, 164 mutants
149 were screened in 12 batches. One mutant *ΔΔhfl1* [orf19.3063] was not screened as it exhibited a severe
150 growth defect on YPD. Each batch included duplicate or triplicate $SN152^+$ controls, for a total of 198
151 cultures and 594 GC-FID runs. Farnesol accumulation values were normalized on a per cell basis using
152 the 50 mL dry weight value of the culture assayed. In this initial screen, the paired WT controls were run
153 a total of 34 times and their whole culture mean E,E-farnesol accumulation value was 5.29 ± 1.12 ng/µL/
154 50 mL dry weight (8.27 ± 2.8 µM).

155 For the rescreen, 27 strains were selected because their farnesol values differed from the
156 average values for $SN152^+$ by a $\log_2$ fold change of > 1.0. To these we added 3 strains (*ΔΔupc2, ΔΔtac1,*
157 *and ΔΔcsr1*) because prior reports from the literature indicated they were likely to have altered farnesol

158 accumulations. These 30 strains were then rescreened five more times, two from the X plate and three
159 from the Y plate (total n =6) in 10 batches including the SN152$^+$ parent in biological duplicate or
160 triplicate, requiring 180 flasks and 540 GC measurements. Thus the rescreen data set examines 30
161 transcriptional regulator mutants (n=6), reporting the means ± SD for normalized farnesol accumulation
162 as detected in whole cultures, pellets, and supernatants as well as the supernatant/pellet ratio.
163 Composite data sets for the initial screen (File S1), rescreen (File S2) and farnesol growth curves (File S3)
164 are available at Figshare. We now describe several highlights from these data sets.
165
166 **Mutants altered in farnesol accumulation**
167 Our initial screen of 164 strains, all from the X plate, was done with an n = 1 comparing whole
168 culture values versus the sum of the cell pellet and supernatant values. The 164 TR mutants were
169 assayed in 12 batches which always included a biological duplicate or triplicate of the SN152$^+$ parent.
170 The whole culture accumulation and supernatant/pellet ratios are shown in Fig. 1. The distribution of
171 the 34 values for SN152$^+$ (red) is shown in Fig. 1 where they can be seen in comparison with the
172 distribution of the 164 TR mutants (black). As expected (Boone et al. 2022), the whole culture (W) and
173 pellet (P) + supernatant (S) values were always very close to one another, with the average WPS relative
174 error values (W-(P+S)/W) being 0.07 ± 0.06 for E,E-farnesol.
175 The vast majority of the 164 TR mutants were unchanged from the SN152$^+$ replicates (Fig. 1).
176 We then identified all mutants which were > 1 $\log_2$ above or below the mean values, as indicated by the
177 4 dotted lines in Fig. 1, and designated them as mutants of interest to be rescreened with greater
178 accuracy. There were 27 mutants with higher or lower farnesol accumulation. Six mutants (*ΔΔcwt1,*
179 *ΔΔrim101, ΔΔcrz2, ΔΔzcf1,ΔΔtea1, ΔΔrme1*) were designated as false positives because their rescreened
180 values from the X and Y plates differed significantly or their rescreen values differed significantly from
181 the initial screen. Thus, we identified ten mutants with elevated farnesol (Fig. 2A), nine with reduced

182 farnesol (Fig. 2B), seven with elevated supernatant/pellet ratios (Fig. 2C), and two with lowered farnesol
183 supernatant/pellet ratios (Fig. 2C). Each of these mutants is described in greater detail in Table 1.
184 Of the 19 mutants with statistically significant differences in farnesol accumulation, only *ΔΔnrg1*
185 had been identified in prior literature (Kebaara et al. 2008). Ten mutants (*ΔΔswi4, ΔΔahr1, ΔΔnrg1,*
186 *ΔΔrap1, ΔΔpho4, ΔΔtye7, ΔΔaaf1, ΔΔash1, ΔΔrtg1, ΔΔssn6*) had significantly increased farnesol
187 accumulation either in the whole culture or supernatant fraction compared to the SN152^{+} parent strain
188 (Table 1). The two highest accumulators (*ΔΔswi4* and *ΔΔahr1)* have known roles in cell cycle progression
189 (Hussein et al. 2011; Sellam et al. 2019). Additionally, two farnesol over accumulating mutants (*ΔΔtye7*
190 and *ΔΔrtg1*) have roles in carbohydrate metabolism (Askew et al. 2011; Moreno-Velásquez et al. 2020),
191 four (*ΔΔahr1, ΔΔnrg1, ΔΔash1, ΔΔssn6*) have a role in dimorphism (Fu et al. 1998; Murad et al. 2001;
192 Inglis and Johnson 2002; García-Sánchez et al. 2005), and two (*ΔΔahr1, ΔΔssn6)* have roles in
193 white/opaque switching (Zordan et al. 2007; Wang et al. 2011; Hernday et al. 2016). *ΔΔwor2* appeared
194 to have a modest increase in accumulation but this did not reach the significance threshold (Table 1, Fig.
195 2A). We note that another regulator of white/opaque switch, Czf1, has role in coordinating switching
196 with the response to farnesol (Langford et al. 2013).
197 Nine mutants (*ΔΔorf19.6874, ΔΔmsn4, ΔΔcph2, ΔΔfcr1, ΔΔsko1, ΔΔgzf3, ΔΔcas5, ΔΔcup9,*
198 *ΔΔtec1*) had significantly decreased farnesol accumulation either in the whole culture or supernatant
199 fraction compared to the SN152^{+} parent strain (Table 1). Three of these low farnesol accumulating
200 mutants (*ΔΔmsn4, ΔΔsko1, ΔΔcas5*) have known roles in stress response to cell wall damage and
201 oxidative stress(Nicholls et al. 2004; Bruno et al. 2006; Rauceo et al. 2008; Xie et al. 2017) and one
202 mutant (*ΔΔcup9*) has a known role in farnesol response by mediating Nrg1 degradation in the absence
203 of farnesol (Lu et al. 2014).
204 The three mutants chosen because of literature precedent had elevated farnesol accumulation
205 but did not reach statistical significance (*ΔΔcsr1, ΔΔupc2, ΔΔtac1*) (Table 1). Ganguly et al. (2011)

206 reported decreased accumulation of farnesol by the *ΔΔcsr1* mutant. Notably, the assay conditions used
207 in our screen (YPD, 30°C) differ significantly from those used in prior studies of *ΔΔcsr1* which employed
208 biofilm forming conditions at 37°C in SPIDER medium (Ganguly et al. 2011). Thus, the dynamics of
209 farnesol accumulation are likely influenced not only by temperature, but also by growth medium (Boone
210 et al. 2022).
211
212 **Mutants altered in the farnesol supernatant/pellet ratio**
213 The supernatant/pellet (S/P) ratios for farnesol were determined for each mutant (n=1) in
214 comparison to those for their $SN152^+$ control (Fig. 1). The value for $SN152^+$ (n= 22 batches) was 0.12 ±
215 0.02 for farnesol. As we had observed previously (Boone et al. 2022), farnesol was predominantly
216 retained in the cell pellet. The S/P ratios were all tightly clustered from 0.07-0.14 except for four
217 mutants (*ΔΔmsn4,ΔΔfcr1, ΔΔgzf3, and ΔΔorf19.6874*) which exhibited less secretion (0.05-0.08) and
218 seven (*ΔΔswi4, ΔΔpho4, ΔΔcas5, ΔΔhap5, ΔΔssn6, ΔΔtye7, and ΔΔrap1*) which exhibited greater
219 secretion (0.19-0.30) (Fig. 2C). Inexplicably, *ΔΔzcf22* was not among the rescreened mutants; it should
220 likely be included among the mutants which exhibited less secretion.
221 Two mutants, *ΔΔhap5* and *ΔΔcas5* are of special interest in that they exhibit greater secretion
222 without being accompanied by greater total farnesol production (Fig. 1). Thus, they target secretion
223 specifically. Mutants such as *ΔΔswi4, ΔΔahr1, and ΔΔrap1* with much greater farnesol production (Fig.
224 2A, Table 1) could exhibit a higher supernatant to pellet ratio because internal and external farnesol are
225 in equilibrium or there is a need to keep internal farnesol levels below a critical threshold value. In both
226 cases, the greater secretion would be an indirect consequence of greater production.
227 **Temporal dynamics of farnesol accumulation**
228 The initial screen and rescreen for farnesol accumulation were done at a single time point 24
229 hours post inoculation. To verify that farnesol differences we observed were not time dependent, we

230 extended the assay to 12, 18, 24, 36, 48, and 80 hours post inoculation for four over accumulating
231 (*ΔΔswi4, ΔΔahr1, ΔΔrap1, ΔΔnrg1*) and two under accumulating (*ΔΔmsn4, ΔΔ19.6874*) mutants (Figs. 3
232 and 4, respectively), with n=2 for each mutant and n=3 for the SN152+ control. Growth of the six mutant
233 strains paralleled the growth of SN152^{+} (Figs. 3A, 4A). As expected, the four over accumulating mutants
234 had elevated farnesol at all time points in both the whole culture (Fig. 3B) and supernatant fractions
235 (Fig. 3D) while the two under accumulating mutants had decreased farnesol in both the whole culture
236 (Fig. 4B) and supernatant fractions (Fig. 4D). To compare total farnesol accumulations, area under the
237 curve analyses (AUC) were performed. The four over accumulating mutants *ΔΔswi4, ΔΔrap1, ΔΔahr1,*
238 and *ΔΔnrg1* had significantly higher AUC in the whole culture (Fig. 3C) and supernatant (Fig. 3E) than the
239 SN152^{+} parent while *ΔΔorf19.6874* and *ΔΔmsn4* had significantly lower supernatant AUC (Fig. 4E). Of
240 great interest, two of the over accumulating mutants (*ΔΔswi4, ΔΔrap1)* still had significant farnesol
241 remaining at 80 hours (Figs. 3B, 3D). They did not exhibit the decay in farnesol levels during stationary
242 phase characteristic of wild type *C. albicans* (Boone et al. 2022) as well as SN152^{+} and the other two over
243 accumulating mutants tested (Fig. 3B), suggesting that a farnesol modification or degradation
244 mechanism is absent from these two mutants.
245
246 **Opaque phenotype of *ΔΔtup1***
247 One surprising result of the screen (Fig. 1) was that *ΔΔtup1* did not appear to over accumulate
248 farnesol in these assay conditions (Table 1). This result was surprising because we had previously
249 reported that the *ΔΔtup1* mutant produced 17 times more farnesol than its parent (Kebaara et al. 2008).
250 A possible explanation for this discrepancy is that *C. albicans* can undergo phenotypic switching
251 between two heritable states: white and opaque, each of which is normally stable for thousands of cell
252 divisions. Switching between the two cell types is reversible and occurs without any chromosomal
253 rearrangements or sequence changes. Critically, Tup1 is a key repressor of the opaque state and

254 Alkafeef et al. (2018) have shown that loss of *TUP1* is sufficient to induce the opaque phase, even in a
255 MTL a/α background (Alkafeef et al. 2018). The pressure of *ΔΔtup1* to spontaneously convert to the
256 opaque phase is strong (Alkafeef et al. 2018) and we already know that wild type opaque cells usually
257 produce far less farnesol than do white cells (Dumitru et al. 2007). Given this, we investigated whether
258 the *ΔΔtup1* mutant in the Homann collection is in the opaque phase under the assay conditions
259 performed in the screen (YPD, 30°*C*). It is important to note that *ΔΔtup1* cells are locked in the
260 filamentous morphology (Kebaara et al. 2008), making visual determination between white and opaque
261 cells more difficult. When plated on YPD medium supplemented with phloxine B and incubated at 30°C,
262 the *ΔΔtup1* colonies were pink while the SN152^{+} colonies plated under the same conditions were white
263 (Fig. 5A). The pink colonies for *ΔΔtup1* are consistant with the cells being in the opaque phase. This view
264 was supported by microscopic examination of the *ΔΔtup1* cells which showed numerous short but
265 elongated cells consistent with the opaque state (Fig. 5B). The typical budding yeast cells of SN152^{+} are
266 included for comparison (Fig. 5B). We are currently investigating the conditions that influence the
267 farnesol production by white and opaque *ΔΔtup1* cells.

268 **Discussion**

269 We examined 164 independent transcriptional regulator knockout mutants for their
270 accumulation and secretion of farnesol. This project was undertaken to define the genes needed for
271 farnesol's synthesis, secretion, and regulation. For logistical reasons, the initial screen and rescreen
272 cultures were grown at 30°C in liquid YPD medium and sampled after 24 hours when the cells were in
273 early stationary phase. The 24 hour time point was chosen based on our prior measurements with wild
274 type *C. albicans* SC5314 over 72 hours of culture which showed that farnesol accumulation generally
275 followed increased cell mass, peaked in early stationary phase, and then declined sharply after ~ 30
276 hours (Boone et al. 2022). Thus, the 24 hour time point was intended to cover the peak of farnesol

277 accumulation. Similarly, our choice of YPD as a growth medium was to insure that all of the TR mutants
278 grew well by 24hrs and indeed 164 out of 165 had done so.
279 With the advantage of now having reliable measures for farnesol presence in whole cultures,
280 cell pellets, and supernatants, we can approach the genetic basis for their synthesis, secretion,
281 regulation, and turnover. As expected, most of the TR mutants were unchanged for these parameters
282 (Fig. 1) while a few potentially useful mutants gave significantly higher and lower levels of farnesol.
283 Significantly, no mutants were entirely devoid of farnesol; its levels often varied but they never dropped
284 to zero. A tentative conclusion from this observation is that farnesol has an essential physiological
285 function over and above acting as a quorum sensing molecule and virulence factor or that it is the
286 product of a redundant biosynthetic pathway. In examing mutants with significant differences in
287 farnesol production, several patterns in the transcriptional networks emerge that may highlight
288 farnesol's physiological functions. These networks include: 1) white-opaque switching, 2) yeast-mycelia
289 dimorphism, 3) response to cell stress, and 4) cell cycle progression. These networks integrate
290 environmental signals to influence the morphology of *C. albicans*. Firstly, three of the transcription
291 regulators studied, Ahr1, Ssn6, and Tup1, have crucial roles in white-opaque switching (Hernday et al.
292 2013; Hernday et al. 2016; Alkafeef et al. 2018). Given that farnesol is toxic to opaque cells (Dumitru et
293 al. 2007), it is intriguing that the *AHR1* deletion mutant over accumulates farnesol while also promoting
294 a higher frequency of white-opaque switching (Hernday et al. 2013). Additionally, it is unclear whether
295 Ssn6 and Ahr1 participate in the response to farnesol, but there is ample precedent given that another
296 transcriptional regulator of the white-opaque switch, Czf1, is involved in farnesol response. Secondly, in
297 addition to Nrg1 and Tup1 (Kebaara et al. 2008), four more transcriptional regulators of yeast-mycelia
298 dimorphism have been demonstrated in this study to influence farnesol accumulation including Cph2,
299 Ash1, Ssn6, and Tec1. Thirdly, *C. albicans* is especially resistant to farnesol compared to other fungi
300 (Semighini et al. 2006; Brasch et al. 2013; Wang et al. 2014), but the mechanism of this tolerance is

301 elusive. One possibility concerns the protective effect of using longer chain ubiquinones (UQ). *C.*
302 *albicans* and *Candida dubliniensis* use UQ9 rather than UQ7 as in other *Candida* species or UQ6 as in *S.*
303 *cerevisiae* (Pathirana et al. 2020). Another possibility could be due to differences in their response to
304 cellular stress. Given that Msn4 and Cas5 have roles in stress response (Nicholls et al. 2004; Xie et al.
305 2017) and influence farnesol accumulation and secretion (Fig. 2), it is likely they may also contribute to
306 farnesol tolerance. Fourthly, cell cycle arrest can also induce filamentous growth of *C. albicans,* either
307 through depletion of cyclins such as Cln3, Clb2, or Clb3 (Bachewich et al. 2005; Bensen et al. 2005),
308 depletion of polo-like kinase Cdc35 (Bachewich et al. 2003), or through treatment with cell cycle
309 inhibitors like hydroxyurea (Bachewich et al. 2005; Chen et al. 2018). Interestingly, expression of the
310 G1/S cyclins *PCL2*, *CLN3*, and *HGC1* are farnesol regulated (Enjalbert and Whiteway 2005). Given that
311 *PLC2* and *CLN3* are Swi4 regulated (Hussein et al. 2011), how these cyclins influence farnesol
312 accumulation is an important question for subsequent studies.
313 There are many questions which can now be approached via the genetic information gleaned
314 from this screen. Among them are: 1/ How is carbon flow through the farnesyl pyrophosphate (FPP)
315 branch point regulated? 2/ Is farnesol made directly from FPP by an appropriate pyrophosphatase (e.g.
316 Dpp1p, Dpp2p, or Dpp3p) or are there other more easily regulated and/or safer biosynthetic pathways?
317 A pathway suggested from *Arabidopsis* invokes the necessary turnover of farnesylated proteins, where
318 proteolytic degradation of those proteins releases farnesylated cysteine which can be cleaved by a ligase
319 to release farnesaldehyde which is then converted to farnesol by a farnesol dehydrogenase (Bhandari et
320 al. 2010). 3/ Is the disappearance of farnesol later in stationary phase due strictly to evaporation of a
321 volatile molecule or to enzymatic conversion of farnesol to, for instance, 2,3-dihydrofarnesol (Brasch et
322 al. 2013; Costa et al. 2020). Significantly, regarding its ability to block germ tube formation and hyphal
323 development, 2,3-dihydrofarnesol is inactive; with only 0.34% of the activity of farnesol (Shchepin et al.
324 2003). This question has now been partially resolved by extending the *ΔΔswi4* and *ΔΔrap1* mutant

325 analyses to 80 hours post inoculation (Fig. 3B). While wild type SC5314 (Boone et al. 2022), SN152^{+}, and
326 most of the mutants examined had little farnesol remaining by 80 hours, *ΔΔswi4* and *ΔΔrap1* differed in
327 that they maintained high levels of farnesol. Clearly, something other than evaporation is occurring.
328 There is ample precedent for farnesol modifying enzymes in fungi. For instance, trans-trans farnesol can
329 be converted to a cis-trans farnesol by *Helminthosporium sativum* (Imai and Marumo 1974).
330 Presumably, the corresponding enzymes for *C. albicans* are not made by *Δswi4* and *ΔΔrap1,* and we are
331 currently using these genetic clues to follow the metabolic disappearance of farnesol during stationary
332 phase.

333 **Author contributions:**

334 DJG: conceptualization, methodology, validation, investigation, writing — original draft, writing —
335 review and editing, visualization, formal analysis, data curation, project administration; JJK: validation,
336 investigation, writing — review and editing; BMT: validation, investigation, writing — review and editing;
337 CHTB: methodology, validation, writing – review and editing; ALA: conceptualization, methodology,
338 resources, supervision, writing — review and editing, project administration; KWN: conceptualization,
339 methodology, resources, supervision, writing — original draft, writing — review and editing, project
340 administration, funding acquisition.

341 **Data availability:**

342 The datasets generated during and/ or analyzed during the current study are available at FigShare. This
343 includes the initial screen (File S1), rescreen dataset (File S2), and farnesol growth curves (File S3).

344 **Acknowledgments:**

345 We are grateful to the Fungal Genetics Stock Center (FGSC) for providing strains, to Prof. Rebecca
346 Roston and Zach Shomo for use and assistance with the gas chromatography system, and to Prof.
347 Haoping Liu for pointing out the possible role of opaque *ΔΔtup1.*

348 **Compliance with ethical standards:**

Funding: This work was supported by Ann L. Kelsall and the Farnesol and *Candida albicans* Research Fund, University of Nebraska Foundation. This research did not receive any specific grant from funding agencies in the public, commercial, or not-for-profit sectors.

Conflict of interest: Daniel J. Gutzmann declares that he has no conflict of interest. Jaxon J. Kramer declares that he has no conflict of interest. Brigid Toomey declares that she has no conflict of interest. Cory H.T. Boone declares that he has no conflict of interest. Audrey L. Atkin declares that she has no conflict of interest. Kenneth W. Nickerson declares that he has no conflict of interest.

Ethical approval: This article does not contain any studies with human participants or animals performed by any of the authors.

373 **References**

374 Alkafeef SS, Yu C, Huang L, Liu H. 2018. Wor1 establishes opaque cell fate through inhibition of the
375 general co-repressor Tup1 in *Candida albicans*. PLoS Genet. 14(1):e1007176.
376 doi:10.1371/journal.pgen.1007176.

377 Alves R, Barata-Antunes C, Casal M, Brown AJP, Van Dijck P, Paiva S. 2020. Adapting to survive: How
378 *Candida* overcomes host-imposed constraints during human colonization. PLoS Pathog. 16(5):e1008478.
379 doi:10.1371/journal.ppat.1008478.

380 Askew C, Sellam A, Epp E, Mallick J, Hogues H, Mullick A, Nantel A, Whiteway M. 2011. The zinc cluster
381 transcription factor Ahr1p directs Mcm1p regulation of *Candida albicans* adhesion. Mol Microbiol.
382 79(4):940–953. doi:10.1111/j.1365-2958.2010.07504.x.

383 Bachewich C, Nantel A, Whiteway M. 2005. Cell cycle arrest during S or M phase generates polarized
384 growth via distinct signals in *Candida albicans*. Mol Microbiol. 57(4):942–959. doi:10.1111/j.1365-
385 2958.2005.04727.x.

386 Bachewich C, Thomas DY, Whiteway M. 2003. Depletion of a polo-like kinase in *Candida albicans*
387 activates cyclase-dependent hyphal-like growth. Mol Biol Cell. 14(5):2163–2180. doi:10.1091/mbc.02-
388 05-0076.

389 Bensen ES, Clemente-Blanco A, Finley KR, Correa-Bordes J, Berman J. 2005. The mitotic cyclins Clb2p and
390 Clb4p affect morphogenesis in *Candida albicans*. Mol Biol Cell. 16(7):3387–3400. doi:10.1091/mbc.e04-
391 12-1081.

392 Bhandari J, Fitzpatrick AH, Crowell DN. 2010. Identification of a Novel Abscisic Acid-Regulated Farnesol
393 Dehydrogenase from *Arabidopsis*. Plant Physiology. 154(3):1116–1127. doi:10.1104/pp.110.157784.

394 Boone CHT, Gutzmann DJ, Kramer JJ, Atkin AL, Nickerson KW. 2022. Quantitative assay for farnesol and
395 the aromatic fusel alcohols from the fungus *Candida albicans*. Appl Microbiol Biotechnol.
396 doi:10.1007/s00253-022-12165-w.

397 Brasch J, Horter F, Fritsch D, Beck-Jendroschek V, Tröger A, Francke W. 2013 Aug. Acyclic sesquiterpenes
398 released by *Candida albicans* inhibit growth of dermatophytes. Med Mycol.:1–10.
399 doi:10.3109/13693786.2013.814174.

400 Bruno VM, Kalachikov S, Subaran R, Nobile CJ, Kyratsous C, Mitchell AP. 2006. Control of the *C. albicans*
401 cell wall damage response by transcriptional regulator Cas5. PLoS Pathog. 2(3):e21.
402 doi:10.1371/journal.ppat.0020021.

403 Chen C, Zeng G, Wang Y. 2018. G1 and S phase arrest in Candida albicans induces filamentous growth via
404 distinct mechanisms. Mol Microbiol. 110(2):191–203. doi:10.1111/mmi.14097.

405 Costa CP, Bezerra AR, Almeida A, Rocha SM. 2020. *Candida* Species (Volatile) Metabotyping through
406 Advanced Comprehensive Two-Dimensional Gas Chromatography. Microorganisms. 8(12):1911.
407 doi:10.3390/microorganisms8121911.

408 Dumitru R, Hornby JM, Nickerson KW. 2004. Defined anaerobic growth medium for studying *Candida*
409 *albicans* basic biology and resistance to eight antifungal drugs. Antimicrob Agents Chemother.
410 48(7):2350–2354. doi:10.1128/AAC.48.7.2350-2354.2004.

411 Dumitru R, Navarathna DHMLP, Semighini CP, Elowsky CG, Dumitru RV, Dignard D, Whiteway M, Atkin
412 AL, Nickerson KW. 2007. In vivo and in vitro anaerobic mating in *Candida albicans*. Eukaryot Cell.
413 6(3):465–472. doi:10.1128/EC.00316-06.

414 Enjalbert B, Whiteway M. 2005. Release from quorum-sensing molecules triggers hyphal formation
415 during *Candida albicans* resumption of growth. Eukaryot Cell. 4(7):1203–1210. doi:10.1128/EC.4.7.1203-
416 1210.2005.

417 Fu Y, Filler SG, Spellberg BJ, Fonzi W, Ibrahim AS, Kanbe T, Ghannoum MA, Edwards JE. 1998. Cloning
418 and characterization of CAD1/AAF1, a gene from *Candida albicans* that induces adherence to endothelial
419 cells after expression in *Saccharomyces cerevisiae*. Infect Immun. 66(5):2078–2084.
420 doi:10.1128/IAI.66.5.2078-2084.1998.

421 Ganguly S, Bishop AC, Xu W, Ghosh S, Nickerson KW, Lanni F, Patton-Vogt J, Mitchell AP. 2011. Zap1
422 control of cell-cell signaling in *Candida albicans* biofilms. Eukaryot Cell. 10(11):1448–1454.
423 doi:10.1128/EC.05196-11.

424 García-Sánchez S, Mavor AL, Russell CL, Argimon S, Dennison P, Enjalbert B, Brown AJP. 2005. Global
425 roles of Ssn6 in Tup1- and Nrg1-dependent gene regulation in the fungal pathogen, *Candida albicans*.
426 Mol Biol Cell. 16(6):2913–2925. doi:10.1091/mbc.e05-01-0071.

427 Gow NAR, van de Veerdonk FL, Brown AJP, Netea MG. 2012. C*andida albicans* morphogenesis and host
428 defence: discriminating invasion from colonization. Nat Rev Microbiol. 10(2):112–122.
429 doi:10.1038/nrmicro2711.

430 Hernday AD, Lohse MB, Fordyce PM, Nobile CJ, DeRisi JL, Johnson AD. 2013. Structure of the
431 transcriptional network controlling white-opaque switching in *Candida albicans*. Mol Microbiol.
432 90(1):22–35. doi:10.1111/mmi.12329.

433 Hernday AD, Lohse MB, Nobile CJ, Noiman L, Laksana CN, Johnson AD. 2016. Ssn6 Defines a New Level of
434 Regulation of White-Opaque Switching in *Candida albicans* and Is Required For the Stochasticity of the
435 Switch. mBio. 7(1):e01565-01515. doi:10.1128/mBio.01565-15.

436 Homann OR, Dea J, Noble SM, Johnson AD. 2009. A phenotypic profile of the *Candida albicans*
437 regulatory network. PLoS Genet. 5(12):e1000783. doi:10.1371/journal.pgen.1000783.

438 Hornby JM, Jensen EC, Lisec AD, Tasto JJ, Jahnke B, Shoemaker R, Dussault P, Nickerson KW. 2001.
439 Quorum sensing in the dimorphic fungus *Candida albicans* is mediated by farnesol. Appl Environ
440 Microbiol. 67(7):2982–2992. doi:10.1128/AEM.67.7.2982-2992.2001.

441 Hussein B, Huang H, Glory A, Osmani A, Kaminskyj S, Nantel A, Bachewich C. 2011. G1/S transcription
442 factor orthologues Swi4p and Swi6p are important but not essential for cell proliferation and influence
443 hyphal development in the fungal pathogen *Candida albicans*. Eukaryot Cell. 10(3):384–397.
444 doi:10.1128/EC.00278-10.

445 Imai K, Marumo S. 1974. Stereochemistry of c-1 hydrogen exchange during a Δ2, 3 trans-cis
446 isomerization of farnesol by *Helminthosporium sativum*. Tetrahedron Letters. 15(49–50):4401–4404.

447 Inglis DO, Johnson AD. 2002. Ash1 protein, an asymmetrically localized transcriptional regulator,
448 controls filamentous growth and virulence of *Candida albicans*. Mol Cell Biol. 22(24):8669–8680.
449 doi:10.1128/MCB.22.24.8669-8680.2002.

450 Kadosh D. 2019. Regulatory mechanisms controlling morphology and pathogenesis in Candida albicans.
451 Curr Opin Microbiol. 52:27–34. doi:10.1016/j.mib.2019.04.005.

452 Kebaara BW, Langford ML, Navarathna DHMLP, Dumitru R, Nickerson KW, Atkin AL. 2008. *Candida*
453 *albicans* Tup1 is involved in farnesol-mediated inhibition of filamentous-growth induction. Eukaryot Cell.
454 7(6):980–987. doi:10.1128/EC.00357-07.

455 Langford ML, Hargarten JC, Patefield KD, Marta E, Blankenship JR, Fanning S, Nickerson KW, Atkin AL.
456 2013. *Candida albicans* Czf1 and Efg1 coordinate the response to farnesol during quorum sensing, white-
457 opaque thermal dimorphism, and cell death. Eukaryot Cell. 12(9):1281–1292. doi:10.1128/EC.00311-12.

458 Lo H-J, Köhler JR, DiDomenico B, Loebenberg D, Cacciapuoti A, Fink GR. 1997. Nonfilamentous C.
459 *albicans* Mutants Are Avirulent. Cell. 90(5):939–949. doi:10.1016/S0092-8674(00)80358-X.

460 Lu Y, Su C, Unoje O, Liu H. 2014. Quorum sensing controls hyphal initiation in *Candida albicans* through
461 Ubr1-mediated protein degradation. Proc Natl Acad Sci U S A. 111(5):1975–1980.
462 doi:10.1073/pnas.1318690111.

463 McCluskey K, Wiest A, Plamann M. 2010. The Fungal Genetics Stock Center: a repository for 50 years of
464 fungal genetics research. J Biosci. 35(1):119–126. doi:10.1007/s12038-010-0014-6.

465 Moreno-Velásquez SD, Tint SH, Del Olmo Toledo V, Torsin S, De S, Pérez JC. 2020. The Regulatory
466 Proteins Rtg1/3 Govern Sphingolipid Homeostasis in the Human-Associated Yeast *Candida albicans*. Cell
467 Rep. 30(3):620-629.e6. doi:10.1016/j.celrep.2019.12.022.

468 Murad AM, Leng P, Straffon M, Wishart J, Macaskill S, MacCallum D, Schnell N, Talibi D, Marechal D,
469 Tekaia F, et al. 2001. NRG1 represses yeast-hypha morphogenesis and hypha-specific gene expression in
470 *Candida albicans*. EMBO J. 20(17):4742–4752. doi:10.1093/emboj/20.17.4742.

471 Neville BA, d'Enfert C, Bougnoux M-E. 2015. *Candida albicans* commensalism in the gastrointestinal
472 tract. FEMS Yeast Research. 15(7):fov081. doi:10.1093/femsyr/fov081.

473 Nicholls S, Straffon M, Enjalbert B, Nantel A, Macaskill S, Whiteway M, Brown AJP. 2004. Msn2- and
474 Msn4-like transcription factors play no obvious roles in the stress responses of the fungal pathogen
475 *Candida albicans*. Eukaryot Cell. 3(5):1111–1123. doi:10.1128/EC.3.5.1111-1123.2004.

476 Noble SM, Gianetti BA, Witchley JN. 2017. *Candida albicans* cell-type switching and functional plasticity
477 in the mammalian host. Nat Rev Microbiol. 15(2):96–108. doi:10.1038/nrmicro.2016.157.

478 Pathirana RU, Boone C, Nickerson KW. 2020. Longer Ubiquinone Side Chains Contribute to Enhanced
479 Farnesol Resistance in Yeasts. Microorganisms. 8(11):1641. doi:10.3390/microorganisms8111641.

480 Pfaller MA, Diekema DJ. 2007. Epidemiology of Invasive Candidiasis: a Persistent Public Health Problem.
481 Clin Microbiol Rev. 20(1):133–163. doi:10.1128/CMR.00029-06.

482 Rauceo JM, Blankenship JR, Fanning S, Hamaker JJ, Deneault J-S, Smith FJ, Nantel A, Mitchell AP. 2008.
483 Regulation of the *Candida albicans* cell wall damage response by transcription factor Sko1 and PAS
484 kinase Psk1. Mol Biol Cell. 19(7):2741–2751. doi:10.1091/mbc.e08-02-0191.

485 Romano A. 1966. Dimorphism. The Fungi, vol. 2. 2:181–209. Academic Press, New York, N.Y.

486 Saville SP, Lazzell AL, Monteagudo C, Lopez-Ribot JL. 2003. Engineered Control of Cell Morphology In
487 Vivo Reveals Distinct Roles for Yeast and Filamentous Forms of *Candida albicans* during Infection.
488 Eukaryot Cell. 2(5):1053–1060. doi:10.1128/EC.2.5.1053-1060.2003.

489 Sellam A, Chaillot J, Mallick J, Tebbji F, Richard Albert J, Cook MA, Tyers M. 2019. The p38/HOG stress-
490 activated protein kinase network couples growth to division in *Candida albicans.* PLoS Genet.
491 15(3):e1008052. doi:10.1371/journal.pgen.1008052.

492 Semighini CP, Hornby JM, Dumitru R, Nickerson KW, Harris SD. 2006. Farnesol-induced apoptosis in
493 *Aspergillus nidulans* reveals a possible mechanism for antagonistic interactions between fungi. Mol
494 Microbiol. 59(3):753–764. doi:10.1111/j.1365-2958.2005.04976.x.

495 Shchepin R, Hornby JM, Burger E, Niessen T, Dussault P, Nickerson KW. 2003. Quorum sensing in
496 *Candida albicans*: probing farnesol's mode of action with 40 natural and synthetic farnesol analogs.
497 Chem Biol. 10(8):743–750. doi:10.1016/s1074-5521(03)00158-3.

498 Wang H, Song W, Huang G, Zhou Z, Ding Y, Chen J. 2011. *Candida albicans* Zcf37, a zinc finger protein, is
499 required for stabilization of the white state. FEBS Lett. 585(5):797–802.
500 doi:10.1016/j.febslet.2011.02.005.

501 Wang X, Wang Y, Zhou Y, Wei X. 2014. Farnesol induces apoptosis-like cell death in the pathogenic
502 fungus *Aspergillus flavus*. Mycologia. 106(5):881–888. doi:10.3852/13-292.

503 Xie JL, Qin L, Miao Z, Grys BT, Diaz JDLC, Ting K, Krieger JR, Tong J, Tan K, Leach MD, et al. 2017. The
504 *Candida albicans* transcription factor Cas5 couples stress responses, drug resistance and cell cycle
505 regulation. Nat Commun. 8(1):499. doi:10.1038/s41467-017-00547-y.

506 Zordan RE, Miller MG, Galgoczy DJ, Tuch BB, Johnson AD. 2007. Interlocking transcriptional feedback
507 loops control white-opaque switching in *Candida albicans*. PLoS Biol. 5(10):e256.
508 doi:10.1371/journal.pbio.0050256.

509

510

511

512

513

514

515

516 **Tables**

517 Table 1. Summary of transcription regulator mutants with statistically significant differences in farnesol
518 accumulation in YPD media at 30°*C.*[a/]

Mutant	*S. cerevisiae* ortholog or best hit from CGD	Mean whole culture E,E-farnesol log_2 fold change vs WT control ± SD (n=6)	Mean supernatant fraction E,E-farnesol log_2 fold change vs WT control ± SD (n=6)	Predicted or known biological process(es) in *Candida albicans* adapted from CGD (Skrzpek et al. 2017)
E,E-farnesol over accumulating mutants				
ΔΔswi4	*SWI4*	2.57*** ± 0.39	3.11*** ± 0.50	Component of SBF complex, G1/S progression
ΔΔahr1	*LYS14*	2.27*** ± 0.42	2.56 ***± 0.32	Regulation of adhesion genes, white/opaque switch, repressor of START
ΔΔnrg1	*NRG2*	1.73*** ± 0.45	1.93*** ± 0.49	Regulator of hyphal gene induction, virulence, chlamydospore formation, stress response
ΔΔrap1	*RAP1*	1.15*** ± 0.62	2.42*** ± 0.48	Telomere maintenance
ΔΔpho4	*PHO4*	1.07*** ± 0.53	1.68*** ± 0.23	Phosphate acquisition
ΔΔtye7	*TYE7*	0.95** ± 0.21	1.83*** ± 0.07	Regulator of glycolysis and carbohydrate metabolism
ΔΔash1	*ASH1*	0.82* ± 0.43	0.92** ± 0.28	GATA-like transcription factor required for WT virulence and filamentous growth
ΔΔaaf1	*none*	0.76* ± 0.31	1.21*** ± 0.19	Expression in *S. cerevisiae* increases adherence
ΔΔrtg1	*RTG1*	0.63 ± 0.49	0.96** ± 0.20	Regulation of sphingolipid homeostasis, galactose catabolism

ΔΔssn6	*CYC8*	0.20 ± 0.90	0.99*** ± 0.73	Forms a corepressor complex with Tup1, regulates a distinct set of genes different than Tup1 in *C. albicans*
ΔΔwor2	*UME6*	0.43 ± 0.82 (p=0.999)	0.59 ± 0.83 (p=0.217)	Regulator of white/opaque switching, maintenance of opaque state
ΔΔtac1 [#]	*HAL9*	0.23 ± 0.56 (p=0.999)	0.36 ± 0.26 (p=0.919)	Transcriptional activator of drug-responsive genes *CDR1* and *CDR2*
ΔΔcsr1 [#]	*ZAP1*	0.32 ± 0.31 (p=0.984)	0.60 ± 0.13 (p=0.195)	Transcription factor, role in zinc homeostasis
ΔΔupc2 [#]	*UPC2*	0.11 ± 0.43 (p=0.999)	0.31 ± 0.46 (p=0.980)	Regulator of ergosterol biosynthetic genes and sterol uptake
ΔΔtup1 [#]	*TUP1*	0.0 ± 0.15 (p=0.999)	-0.02 ± 0.47 (p=0.999)	Transcriptional corepressor with *Ssn6p*, regulates morphological switching, farnesol response, germ tube formation
E,E-farnesol under accumulating mutants				
ΔΔ orf19.6874 (C2_05640 W_A)	*BAS1*	-2.10*** ± 0.73	-2.65*** ± 1.03	Transcription factor, null mutant exhibits increase in invasive growth
ΔΔmsn4	*MSN2*	-1.89*** ± 0.37	-2.40*** ± 0.65	Zinc finger transcription factor, not a significant stress response regulator in *C. ablicans*
ΔΔcph2	*HMS1*	-1.93*** ± 0.63	-2.04*** ± 0.91	Transcriptional activator of hyphal growth
ΔΔfcr1	*CAT8*	-1.97*** ± 0.88	-3.68*** ± 3.83	Negative regulator of fluconazole/ketoconazole/brefeldin A resistance
ΔΔsko1	*SKO1*	-1.93*** ± 0.39	-1.41*** ± 0.46	Cell wall damage response, morphological switching, oxidative stress response
ΔΔgzf3	*GZF3*	-1.32*** ± 0.32	-1.63*** ± 0.54	GATA type transcription factor, ortholog regulates nitrogen catabolic gene expression

ΔΔcas5	*MOT3*	-1.16** ± 0.13	-0.51 ± 0.32	Cell wall homeostasis, adherence, stress response, cell cycle
ΔΔcup9	*TOS8*	-1.08** ± 0.63	-0.85 ± 0.86	Represses SOK1 expression in response to farnesol inhibition
ΔΔtec1	*TEC1*	-0.75* ± 0.66	-0.58 ± 0.76	Hyphal gene regulator, white cell pheromone response

a/ Log_2 fold change production values ± SD represent the mean farnesol accumulation value of 3 X and 3 Y (n=6) independently derived mutant compared to the mean farnesol accumulation value of the paired SN152 parent (n=22. Both over and under accumulating mutants are ordered by how much they exceed the SN152 parent. The four mutants added because of literature precedent are indicated by #. Differences between mutants (n=6) and the $SN152^+$ parent (n=22 batches) were accessed by One-way ANOVA with Dunnett's multiple comparisons test using GraphPad Prism. Differences were considered significant at $p<0.05$ (*$p<0.05$, **$p<0.01$, ***$p<0.001$).

Figure Captions

Fig. 1. Initial screen E,E-farnesol supernatant to pellet ratio vs E,E- farnesol whole culture accumulation at 24 hours post inoculation. Data represents the accumulation values for each of 164 transcription regulator mutants (black) (n=1) and each $SN152^+$ replicate (red) (n=34). The red X indicates the mean value for the $SN152^+$ replicates (n=34). Dotted lines represent a log2 fold change increase or decrease of 1 for farnesol from the mean for $SN152^+$.

Fig. 2. Transcription regulator mutants differing in farnesol accumulation and localization. Accumulation values were measured 24 hours post inoculation at 30°C in YPD for each transcription regulator mutant in both the X (3) and Y (3) independent mutants (total n=6) and the $SN152^+$ parent (n=22 batches). Data represents the mean accumulation value ± SD (A,B) or mean farnesol supernatant to pellet ratio ± SD (C). The mutants added because of literature precedent are indicated by #. Differences between groups that were normally distributed and that had equal variances (C) were accessed by One-way ANOVA with Dunnett's multiple comparisons test. Differences between groups that were not normally distributed or

541 heteroscedastic (A,B) were accessed by Kruskal-Wallis test with Dunn's multiple comparisons tests.

542 Differences were considered significant at $p<0.05$ (*$p<0.05$, **$p<0.01$, ***$p<0.001$).

543

544 **Fig. 3.** Temporal dynamics of farnesol accumulation in *ΔΔswi4, ΔΔahr1, ΔΔrap1, and ΔΔnrg1.* Farnesol

545 accumulation was accessed at 12, 18, 24, 36, 48, 80 hours post inoculation at 30°C in YPD for each

546 transcription regulator mutant in two independent growth curves (n=2) and 3 independent growth

547 curves for $SN152^{+}$ (n=3). Dry weights were accessed as each time point and are presented as the mean

548 dry weight ± SEM (A). Farnesol accumulation data represents the mean dry weight normalized farnesol

549 accumulation value ± SEM in either the whole culture (B) or the supernatant fraction (D). To access

550 overall farnesol production, area under the curve analyses (AUC) were performed and data are the

551 mean AUC ± SE for the whole culture (C) or supernatant fraction (E). Differences in the AUC between

552 groups were accessed by One-way ANOVA with Dunnett's multiple comparisons test. Differences were

553 considered significant at $p<0.05$ (*$p<0.05$, **$p<0.01$, ***$p<0.001$).

554 **Fig. 4.** Temporal dynamics of farnesol accumulation in *ΔΔorf19.6874, and ΔΔmsn4.* Farnesol

555 accumulation was accessed at 12, 18, 24, 36, 48, 80 hours post inoculation at 30°C in YPD for each

556 transcription regulator mutant in two independent growth curves (n=2) and 3 independent growth

557 curves for $SN152^{+}$ (n=3). Dry weights were accessed as each time point and are presented as the mean

558 dry weight ± SEM (A). Farnesol accumulation data represents the mean dry weight normalized farnesol

559 accumulation value ± SEM in either the whole culture (B) or the supernatant fraction (D). To access

560 overall farnesol production, area under the curve analyses (AUC) were performed and data are the

561 mean AUC ± SE for the whole culture (C) or supernatant fraction (E). Differences in the AUC between

562 groups were accessed by One-way ANOVA with Dunnett's multiple comparisons test. Differences were

563 considered significant at $p<0.05$ (*$p<0.05$, **$p<0.01$, ***$p<0.001$).

564

565 **Fig. 5.** Characterization of *ΔΔtup1* morphology in conditions used for the screen. (A) Representative

566 micrographs of the colony morphology of SN152^{+} (white) and *ΔΔtup1* (pink) on YPD agar supplemented

567 with phloxine B grown at 30°C . (B) Representative micrographs of cellular morphology of SN152^{+} (yeast)

568 and *ΔΔtup1* (hyphae and elongated cells).

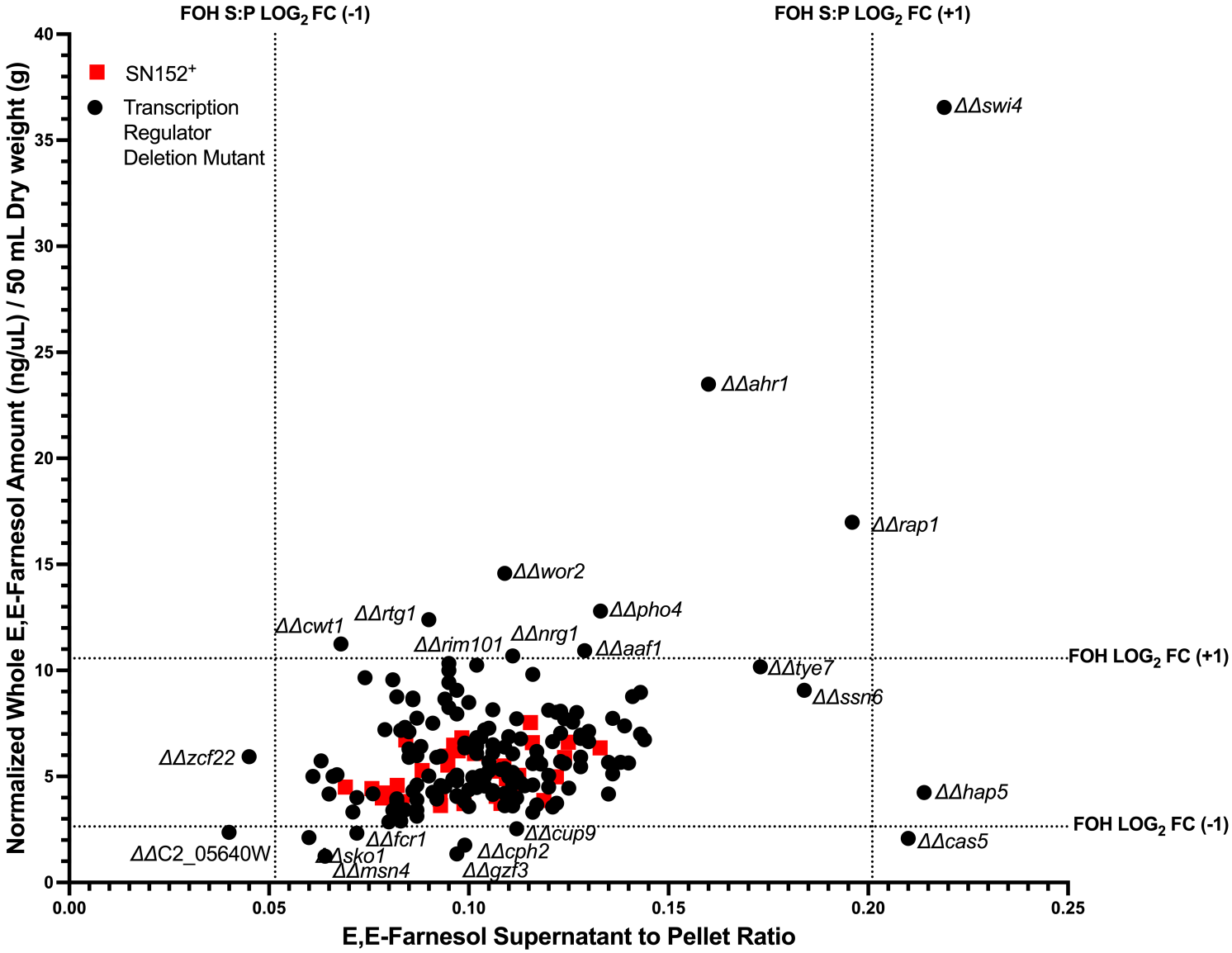
FOH S:P LOG2 FC (-1)
FOH S:P LOG2 FC (+1)
SN152+
Transcription Regulator Deletion Mutant
ΔΔswi4
ΔΔahr1
ΔΔrap1
ΔΔwor2
ΔΔpho4
ΔΔrtg1
ΔΔcwt1
ΔΔrim101
ΔΔnrg1
ΔΔaaf1
ΔΔtye7
ΔΔssn6
ΔΔzcf22
ΔΔhap5
ΔΔcup9
ΔΔfcr1
ΔΔC2_05640W
Δsko1
ΔΔcph2
ΔΔcas5
ΔΔmsn4
ΔΔgzf3
FOH LOG2 FC (+1)
FOH LOG2 FC (-1)
Normalized Whole E,E-Farnesol Amount (ng/uL) / 50 mL Dry weight (g)
E,E-Farnesol Supernatant to Pellet Ratio
0
5
10
15
20
25
30
35
40
0.00
0.05
0.10
0.15
0.20
0.25

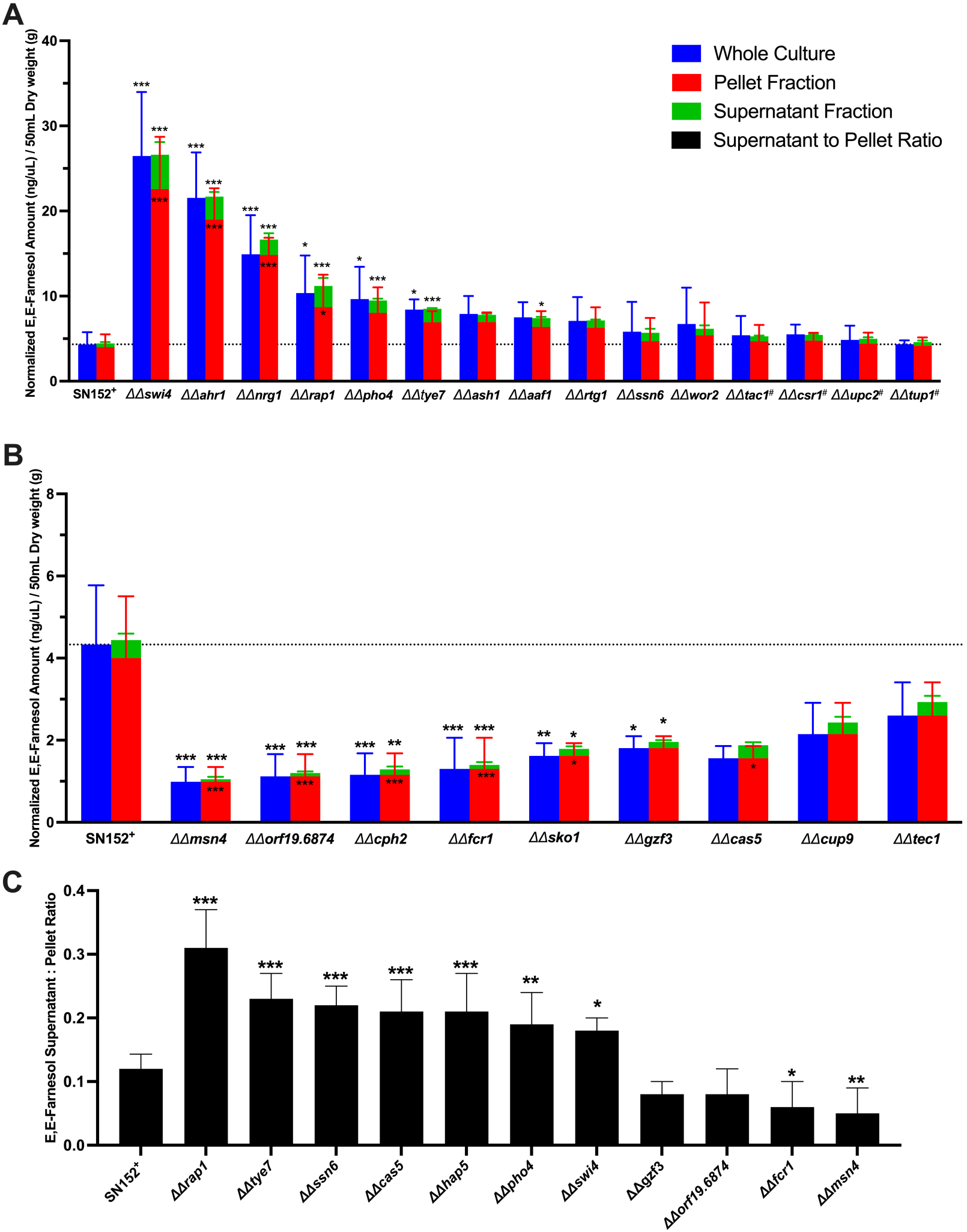
A
Normalized E,E-Farnesol Amount (ng/uL) / 50mL Dry weight (g)
Whole Culture
Pellet Fraction
Supernatant Fraction
Supernatant to Pellet Ratio
SN152+
ΔΔswi4
ΔΔahr1
ΔΔnrg1
ΔΔrap1
ΔΔpho4
ΔΔtye7
ΔΔash1
ΔΔaaf1
ΔΔrtg1
ΔΔssn6
ΔΔwor2
ΔΔtac1#
ΔΔcsr1#
ΔΔupc2#
ΔΔtup1#
B
Normalized E,E-Farnesol Amount (ng/uL) / 50mL Dry weight (g)
SN152+
ΔΔmsn4
ΔΔorf19.6874
ΔΔcph2
ΔΔfcr1
ΔΔsko1
ΔΔgzf3
ΔΔcas5
ΔΔcup9
ΔΔtec1
C
E,E-Farnesol Supernatant : Pellet Ratio
SN152+
ΔΔrap1
ΔΔtye7
ΔΔssn6
ΔΔcas5
ΔΔhap5
ΔΔpho4
ΔΔswi4
ΔΔgzf3
ΔΔorf19.6874
ΔΔfcr1
ΔΔmsn4

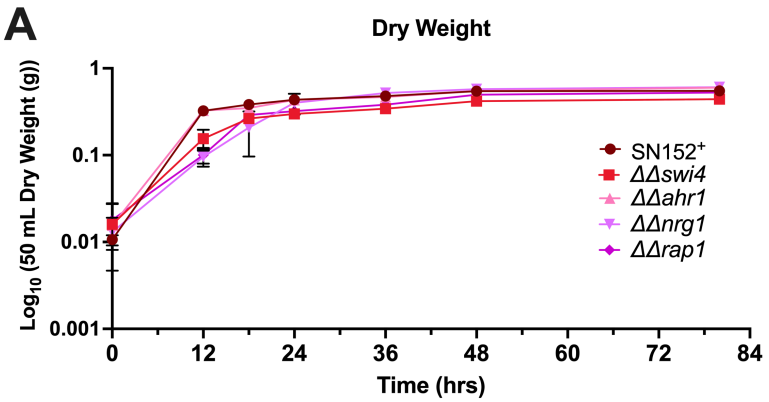
A
Dry Weight
Log10 (50 mL Dry Weight (g))
1
0.1
0.01
0.001
0
12
24
36
48
60
72
84
Time (hrs)
SN152+
ΔΔswi4
ΔΔahr1
ΔΔnrg1
ΔΔrap1

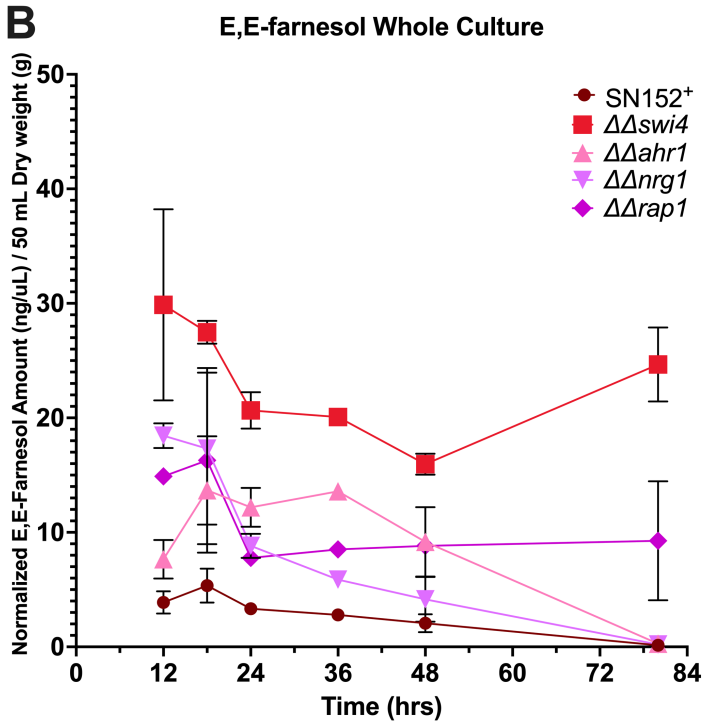
B
E,E-farnesol Whole Culture
Normalized E,E-Farnesol Amount (ng/uL) / 50 mL Dry weight (g)
50
40
30
20
10
0
0
12
24
36
48
60
72
84
Time (hrs)
SN152+
ΔΔswi4
ΔΔahr1
ΔΔnrg1
ΔΔrap1

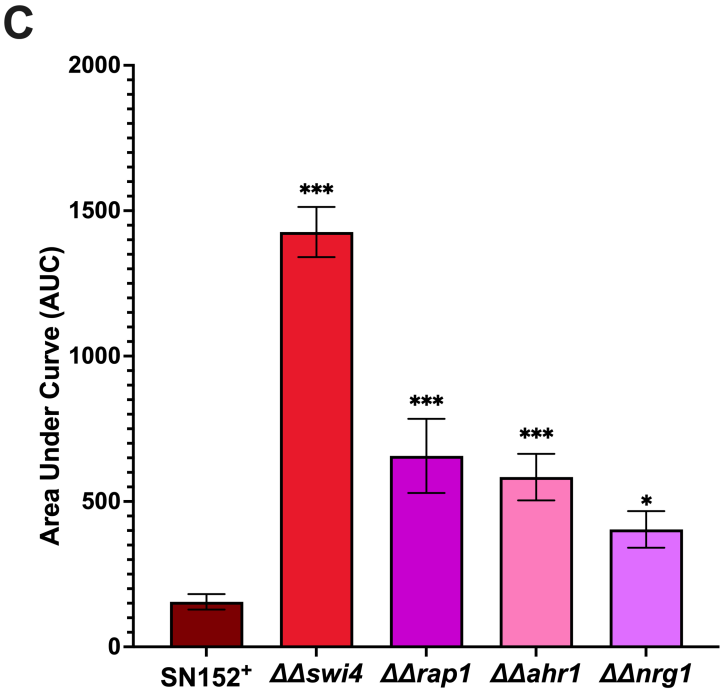
C
Area Under Curve (AUC)
2000
1500
1000
500
0
***
***
***
*
SN152+
ΔΔswi4
ΔΔrap1
ΔΔahr1
ΔΔnrg1

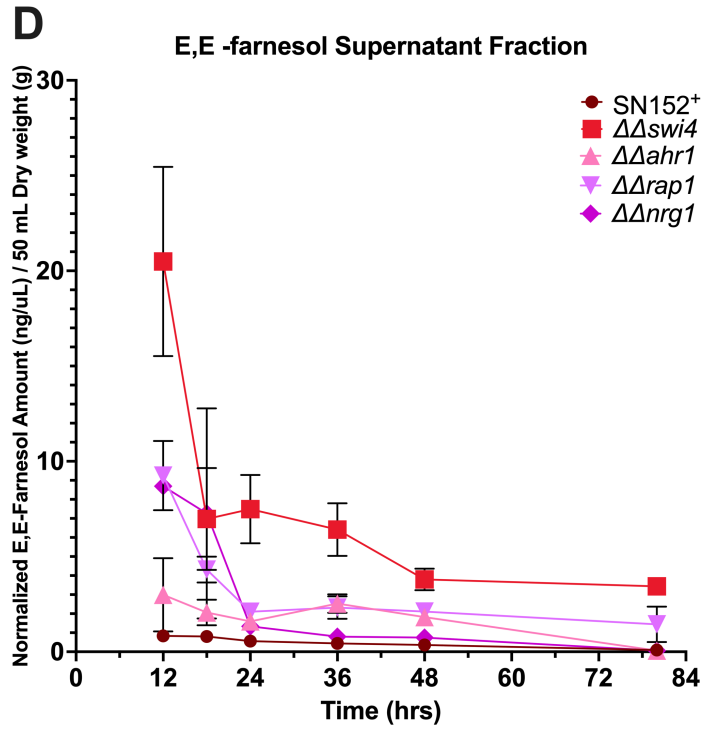
D
E,E -farnesol Supernatant Fraction
Normalized E,E-Farnesol Amount (ng/uL) / 50 mL Dry weight (g)
30
20
10
0
0
12
24
36
48
60
72
84
Time (hrs)
SN152+
ΔΔswi4
ΔΔahr1
ΔΔrap1
ΔΔnrg1

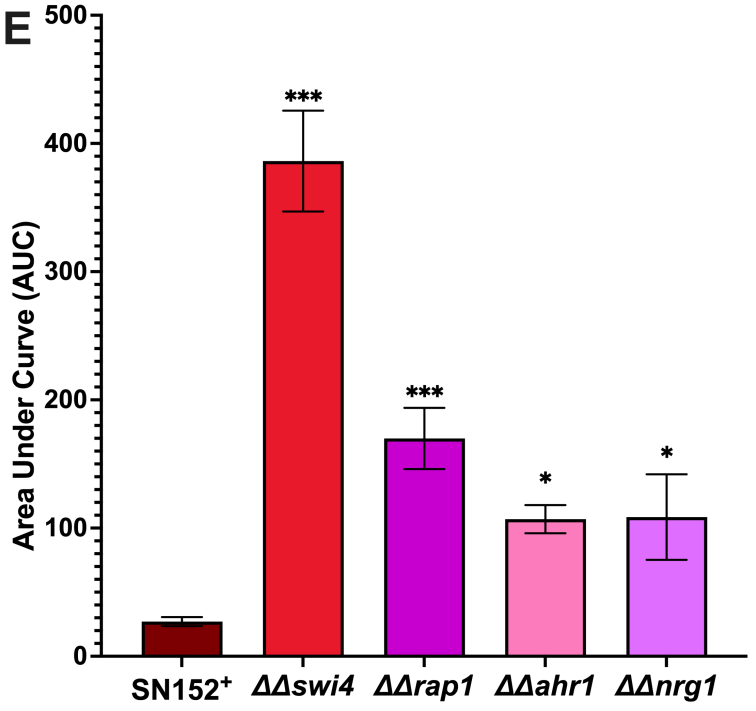
E
Area Under Curve (AUC)
500
400
300
200
100
0
***
***
*
*
SN152+
ΔΔswi4
ΔΔrap1
ΔΔahr1
ΔΔnrg1

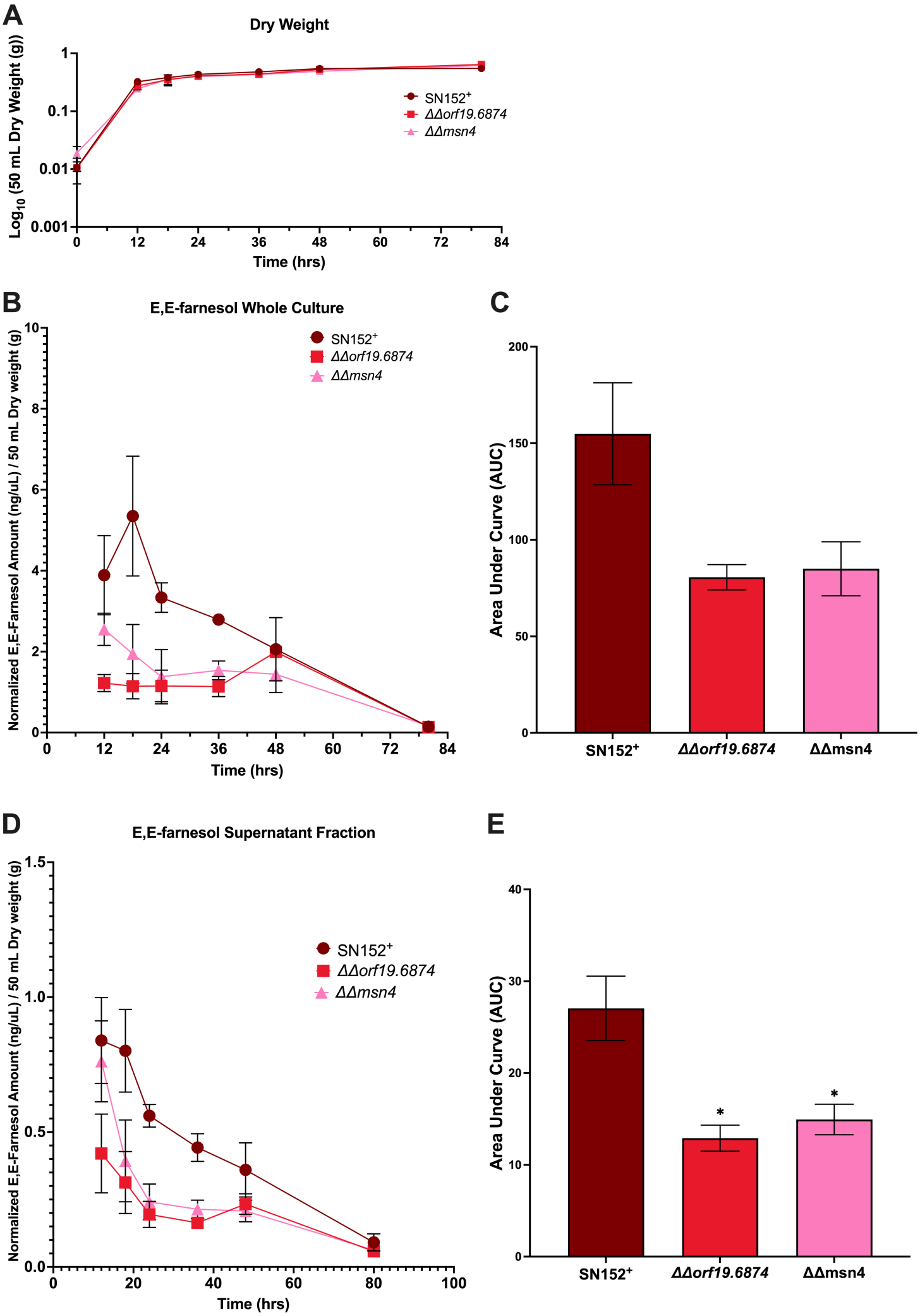
A
Dry Weight
Log10 (50 mL Dry Weight (g))
1
0.1
0.01
0.001
0
12
24
36
48
60
72
84
Time (hrs)
SN152+
ΔΔorf19.6874
ΔΔmsn4
B
E,E-farnesol Whole Culture
Normalized E,E-Farnesol Amount (ng/uL) / 50 mL Dry weight (g)
10
8
6
4
2
0
Time (hrs)
SN152+
ΔΔorf19.6874
ΔΔmsn4
C
Area Under Curve (AUC)
200
150
100
50
0
SN152+
ΔΔorf19.6874
ΔΔmsn4
D
E,E-farnesol Supernatant Fraction
Normalized E,E-Farnesol Amount (ng/uL) / 50 mL Dry weight (g)
1.5
1.0
0.5
0.0
0
20
40
60
80
100
Time (hrs)
SN152+
ΔΔorf19.6874
ΔΔmsn4
E
Area Under Curve (AUC)
40
30
20
10
0
*
*
SN152+
ΔΔorf19.6874
ΔΔmsn4

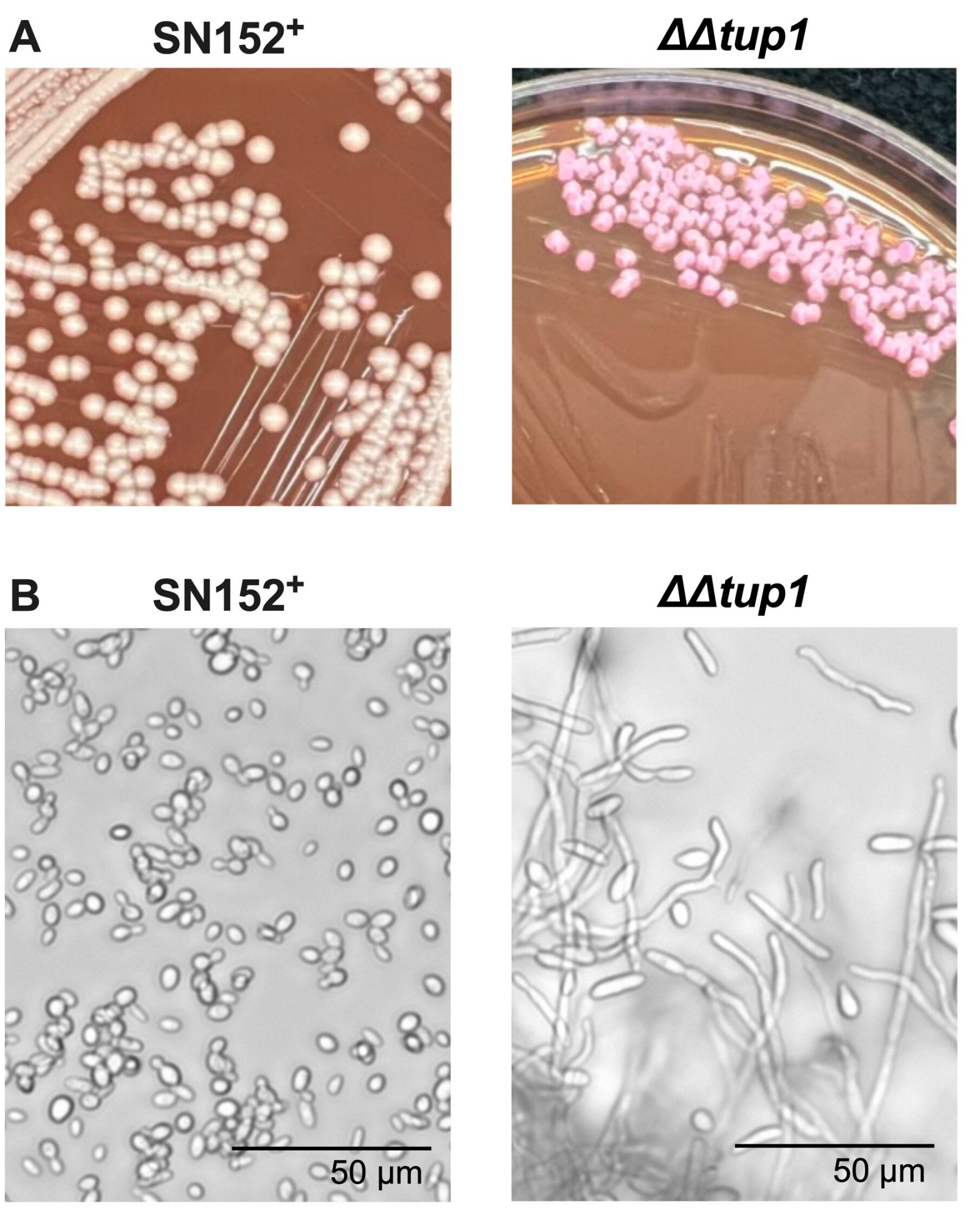
A
SN152+
ΔΔtup1
B
SN152+
ΔΔtup1
50 µm
50 µm